Avrupa Bilim ve Teknoloji Dergisi
Özel Sayı 40, S. 67-74, Eylül 2022

Araştırma Makalesi

www.ejosat.com ISSN:2148-2683

European Journal of Science and Technology
Special Issue 40, pp. 67-74, September 2022

Research Article

A Detection and Prediction Model Based on Deep Learning Assisted by Explainable Artificial Intelligence for Kidney Diseases

Ahmet Furkan Bayram[1], Caglar Gurkan[2,*], Abdulkadir Budak[3] and Hakan Karatas[4]

[1] Department of Computer Engineering, Faculty of Engineering, Karadeniz Technical University, Trabzon (ORCID: 0000-0002-1304-9941), bayramahmet48@gmail.com

[2*] Department of Electrical and Electronics Engineering, Graduate School of Science, Eskisehir Technical University, Eskisehir, (ORCID: 0000-0002-4652-3363), caglargurkan@eskisehir.edu.tr

[2*] Department of Artificial Intelligence and Image Processing, Akgun Computer Inc., Ankara (ORCID: 0000-0002-4652-3363), caglar.gurkan@akgun.com.tr

[3] Department of Artificial Intelligence and Image Processing, Akgun Computer Inc., Ankara (ORCID: 0000-0002-0328-6783), kadir.budak@akgun.com.tr

[4] Department of Artificial Intelligence and Image Processing, Akgun Computer Inc., Ankara (ORCID: 0000-0002-9497-5444), hakan.karatas@akgun.com.tr

(1st International Conference on Innovative Academic Studies ICIAS 2022, September 10-13, 2022)

(**DOI:** 10.31590/ejosat.1171777)

ATIF/REFERENCE: Bayram, A.F., Gurkan, C., Budak, A. & Karatas, H. (2022). A Detection and Prediction Model Based on Deep Learning Assisted by Explainable Artificial Intelligence for Kidney Diseases. *European Journal of Science and Technology*, (40), 67-74.

Abstract

Kidney diseases are one of the most common diseases worldwide and cause unbearable pain in most people. In this study aims to detecting the cyst and stone in the kidney. For the this purpose, YOLO architecture designs were used for detection of kidney, kidney cyst and kidney stone. The YOLO architecture designs were supported by the explainable artificial intelligence (xAI) feature. CT images in three classes, namely 72 kidney cysts, 394 kidney stones and 192 healthy kidneys were used in the performance analysis part of the YOLO architecture designs. As a result, YOLOv7 architecture design outperformed the YOLOv7 Tiny architecture design. YOLOv7 architecture design achieved the mAP50 of 0.85, precision of 0.882, sensitivity of 0.829 and F1 score of 0.854. Consequently, deep learning based xAI assisted computer aided diagnosis (CAD) system was developed for diagnosis of kidney diseases.

Keywords: Kidney stone, Kidney cyst, Deep learning, YOLOv7, Explainable artificial intelligence.

Böbrek Hastalıkları için Açıklanabilir Yapay Zeka Destekli Derin Öğrenmeye Dayalı Bir Tespit ve Tahmin Modeli

Öz

Böbrek hastalıkları dünya çapında en yaygın hastalıklardan biridir ve çoğu insanda dayanılmaz ağrılara neden olur. Bu çalışmada böbrekteki kist ve taşın tespiti amaçlanmıştır. Bu amaçla böbrek, böbrek kisti ve böbrek taşı tespiti için YOLO mimari tasarımları kullanılmıştır. YOLO mimari tasarımları açıklanabilir yapay zeka (AYZ) özelliği ile desteklenmiştir. YOLO mimari tasarımlarının performans analizi kısmında 72 böbrek kisti, 394 böbrek taşı ve 192 sağlıklı böbrek olmak üzere üç sınıftaki BT görüntüleri kullanılmıştır. Sonuç olarak, YOLOv7 mimari tasarımı, YOLOv7 Tiny mimari tasarımından daha iyi performans gösterdi. YOLOv7 mimari tasarımı 0.85 mAP50 değerini, 0.882 kesinliği, 0.829 duyarlılığı ve 0.854 F1 skorunu elde etmiştir. Sonuç olarak, böbrek hastalıklarının teşhisi için derin öğrenme tabanlı AYZ destekli bilgisayar destekli tanı (BDT) sistemi geliştirilmiştir.

Anahtar Kelimeler: Böbrek taşı, Böbrek kisti, Derin öğrenme, YOLOv7, Açıklanabilir yapay zeka.

[*] Corresponding Author: caglar.gurkan@akgun.com.tr

1. Introduction

Kidney pain is one of the most common complaints, although the rate of complaints in emergency and clinical presentations varies. In prevalence studies (Türk et al., 2016; Stamatelou et al., 2003), it is seen that this rate reaches up to 20% and is increasing gradually. The incidence of kidney stones in people aged 20 to 74 living in the United States (US) is approximately 9% (Scales et al., 2012). The probability of coming to the emergency department with the complaint of kidney stones is critical level. This number is seen to reach 1,000,000 every year in the US, additionaly this number has doubled between 1992 and 2009 (Fwu et al., 2013). At the same time, the incidence of this disease was higher between 1988 and 1994 than between 1976 and 1980. It has been observed that this rate gradually increased between 2007 and 2016 (Chewcharat & Curhan, 2021).

Nowadays, artificial intelligence (AI) is intended to be primarily used in the field of medicine. Several researches have been carried out in various fields by using images in the medical field together with the deep learning and machine learning techniques. These techniques have been successfully used in segmentation of medical images (Weston et al., 2019), classification of diseases (Ozturk et al., 2020), lesion detection (Yan et al., 2018) and in many other fields. Medical products and services are products that must be of high reliability. To fully trust these products, knowing why artificial intelligence makes its decisions is the most important step. While providing a high level of learning performance with explainable AI (xAI), it also explains why the decision was made. In this way, the reason for the decision can be questioned and its correctness can be discussed in a better way. Recently, AI based studies have been performed in many areas such as the treatment process of diseases in the human body (Z. Lin et al., 2021). The main purpose of AI assisted diagnosis is to develop systems that enable radiologists to assist in the detection of disease. Examples of these systems are kidney segmentation (D. T. Lin et al., 2006), cyst segmentation (Z. Lin et al., 2021), kidney stone segmentation (Baygin et al., 2022), systems that classify the computerized tomography image according to its condition (Z. Lin et al., 2021).

Choosing an accurate imaging method for the detection of kidney stones and cysts is of vital importance as it is the first step of treatment. Non-contrast computed tomography (CT) of the abdomen provides the most accurate diagnosis, but exposes the patient to radiation. Ultrasonography, on the other hand, has lower sensitivity than CT, but its advantage is that no radiation is used in its use. In MR imaging method, it uses the 3D imaging method, but this method is both costly and difficult to evaluate kidney stones (Weston et al., 2019). Therefore, computer aided diagnosis (CAD) has been developed to find kidney stones and cysts to give advice to radiologists. Correctly determining the location of the kidney stone and cyst is an important preliminary step. Thanks to the correct determination to be made, it will provide quantitative information to pay attention to the stones that will be missed. These systems, which automatically detect them and show their locations, provide great convenience to radiologists.

In this study, a model was designed supported by xAI to detect physician-induced small stones and cysts that are difficult to distinguish, using CT images.

The main purpose of this study, to save time and to minimize the error rate in the determinations originating from the physician by contributing to long-term disease analysis procedures.

The contributions of this proposed study are outlined as follows:

1. A open source data set was labelled in three-classes, such as kidney, kidney stone, and kidney cyst.

2. The developed AI model assited by xAI.

3. The AI assisted diagnosis system has been developed, with the use of developed system can be reduce the workload of health employees.

The rest of this paper is organized as follows. In Section 2, related researches based on segmentation and detection for the diagnose of kidney diseases have been reported. In Section 3, the utiliezed methodologies have been detailed. In Section 4, obtained results have been discussed. In Section 5, concluding remarks have been reported.

2. Related Works

It has been suggested by many scientific researchers that several segmentation and detection techniques can be used for kidney diseases.

Ruberto et al. (Ruberto et al., 2022) aimed to perform kidney and kidney stone segmentation using CT images. 3-dimensional segmentation approaches were used in the study. The used data set consists of CT images of 260 patients. In the segmentation task, state-of-the-art networks in the literature such as DeepLabV3+, SegNet, 3D U-Net, UNET and Res U-NET were used. The best segmentation performance was obtained by RES U-NET network in the comparative analysis. Dice similarity coefficient (DSC) of 96.54% and 96.54% were achieved for kidney and kidney stone segmentations, respectively.

Lin et al. (Z. Lin et al., 2021) aimed to perform kidney and renal tumor segmentation using CT images. 3D U-NET segmentation network was used in the study. The used data set consists of CT images of 476 patients. The segmentation accuracy was analyzed with the DSC. DSC of 97.3% and 84.4% results were achieved for kidney and renal tumor, respectively.

Yildirim et al. (Yildirim et al., 2021) proposed the method for classification of CT images with deep learning technique using CT images from coronal view. The used data set consist of 1799 images. Accuracy of 96.82% was achieved for detecting the kidney stones.

Baygin et al. (Baygin et al., 2022) aimed to classify patients with or without kidney stones using CT images. The used data set consists of CT images of 433 patients. In the study, a novel classification network called ExDark19 was proposed. The classification network was trained by using the transfer learning method. K nearest neighbor (kNN) algorithm was used as classifier. The classification accuracy of 99.22% was achieved.

Cui et al. (Cui et al., 2021) aimed to perform kidney stone detection and segmentation using CT images. The used data set consists of CT images of 167 and 282 patients for segmentation and for classification tasks, respectively. In the study, a novel method called S.T.O.N.E was proposed for classification task. In segmentation task, 3D U-NET segmentation network was used. DSC of 97% was achieved.

Fu et al. (Fu et al., 2021) aimed to perform the segmentation of chronic diseases in the kidney using CT images. The used data set consists of CT images of 79 patients. RDA U-NET segmentation network was used for segmentation. DSC of 97.3% was achieved.

3. Methodology

The utilized methodology in the study is presented under the subtitles data set, detection algorithms, xAI, and performance evaluation metrics.

3.1. Data set

The data set was collected from PACS from different hospitals in Dhaka, Bangladesh. The data set includes patients diagnosed with namely kidney cyst, normal and stone findings. This data set consists of coronal, axial and sagittal images, but axial images were used in this paper. The data set consist of total of 1,280 non-contrast CT images in three classes, such as 494 images of kidney stones, 498 images of kidney cysts, and 288 images of normal kidney (Islam et al., 2022). Further, training, validation, and testing sizes constitutes of %75, %10, and %15 of the total size, respectively.

Since this data set was used in the image classification task, it does not contain any masks. Therefore, after the have a high image resolution images were selected in this data set, the labeling process was carried out in this research. Make Sense which is web-based image annotation tool was used in labelling step (Make Sense, n.d.).

3.2. Detection Algorithms

In this study, YOLOv7 and YOLOv7 Tiny architecture designs were used in order to compare the performances in the detection of kidney diseases. YOLO architecture designs are instead of selecting some regions in the image, it detects regions in the image and apply a neural network to the entire image to draw bounding boxes around it. YOLO architecture designs are a single deep convolutional neural network which are the dividing the input image into grids. The architecture designs have an associated vector that reports whether there is any desired object in that grid. On the other hand, since these architecture designs are a progressive model, its learning improves over time and gives more accurate results. The working mechanism of the architecture designs is to hold the object with the highest accuracy rate among the objects detected in that region and discard the rest (Gothane, n.d.).

Training phase for YOLO architecture designs are as follows:

Adam optimizer was used for weights updates, cross entropy was used as loss function, and learning rate was selected as 1e-3. YOLO architecture designs were trained along 150 epoch while batch size was set as 8. All experiments were implemented in Pytorch library and Google Colab integrated development environment (IDE) by using NVIDIA Tesla P100 graphics card.

3.3. xAI

Medical products and services are built on high trust and conditions. New generation medical software is used to provide this high level of trust. Nowadays, artificial intelligence is expected to be used in medical fields and studies are being carried out on it. The main reason for using these software is that it helps to save the time problem. However, AI is not efficiently explained the decisions and results. Additionaly, users must be able to understand the implications of AI and decide when to trust it and when not to. Regardless, xAI-powered decision support systems enable users to highly trust AI (Dosilovic et al., 2018; Selvaraju et al., 2017; Selvaraju et al., 2016).

3.4. Performance Evulation Metrics

The mean average precision (mAP) performance evaluation metric was used to analyze the accuracy of the YOLO architecture designs in the study. Firstly, the Intersection over Union (IoU) performance evaluation metric is calculated for calculating the AP value in detection tasks. The IoU value is calculated by the ratio of the union area of the predicted and actual bounding boxes to the overall area. The Average Sensitivity or mAP score is calculated by taking the mean AP over all classes and/or overall IoU thresholds based on the different detection difficulties.

True Positive (TP): If the IoU value is greater than 0.5, it is evaluated in this part.

False Positive (FP): If the IoU value is less than 0.5 or the two or more bounding boxes are created for a object, it is evaluated in this part.

False Negative (FN): If no object is detected or if its class is incorrect when the IoU value is greater than 0.5, it is evaluated in this part.

Precision and sensitivity parameters are calculated using TP, FP and FN parameters. The precision, sensitivity, F1-score formulas are shown in Equation 1, Equation 2 and Equation 3, respectively. In this study, the threshold value of IoU was set as 0.5.Equation 2, respectively. In this study, the threshold value of IoU was set as 0.5.

$$\text{Precision (PRE)} = TP/(TP+FP) \quad (1)$$

$$\text{Sensitivity (STV)} = TP/(TP+FN) \quad (2)$$

$$\text{F1-Score} = 2*(PRE*STV)/(PRE+ STV) \quad (3)$$

4. Results and Discussion

The results and discussion is presented under the subtitles results obtained by YOLOv7, results obtained by YOLOv7 Tiny, outputs of xAI.

4.1. Result Obtained By YOLOv7

Table 1 represents the results obtained by using the YOLOv7. The mAP50 of 85%, precision of 88.2%, sensitivity of 82.9% and F1 score of 85.4% values were achieved by YOLOv7 for average of all classes. The mAP0.5 of 97.3%, precision of 93.6%, sensitivity of 100% and F1 score of 96.6% values were achieved by YOLOv7 for kidney class. The mAP0.5 of 84.9%, precision of 81.9%, sensitivity of 85.5% and F1 score of 83.6% values were achieved by YOLOv7 for kidney stone class. The mAP0.5 of 72.7%, precision of 89.2%, sensitivity of 63.3% and F1 score of 74% values were achieved by YOLOv7 for kidney cyst class. The training period of the model took 4 hours and 10 minutes.

Table 1. Results obtained by YOLOv7

Classes	mAP50	PRE	STV	F1-Score
Kidney	97.3%	93.6%	100%	96.6%
Kidney Stone	84.9%	81.9%	85.5%	83.6%
Kidney Cyst	72.7%	89.2%	63.3%	74%
Average	85%	88.2%	82.9%	85.4%

From Figure 1, considering the confusion matrix values, the classification accuracy values 0.92, 1.0, and 0.54 for kidney stones, kidney, and kidney cyst, respectively.

Precision is a measure of result relevance, while recall is a measure of how many truly relevant results were returned. From Figure 2, the average precision-recall values were achieved as 0.833, 0.976, 0.488, 0.766 for kidney stone, kidney, kidney cyst, and all classes.

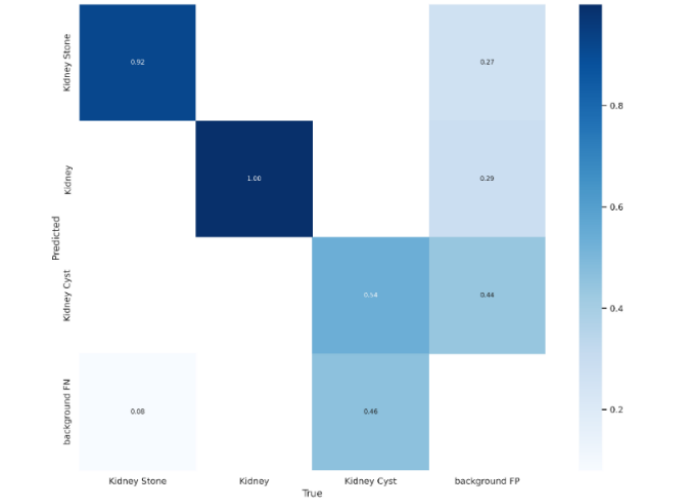

Figure 1. Obtained confusion matrix by using YOLOv7 architecture design

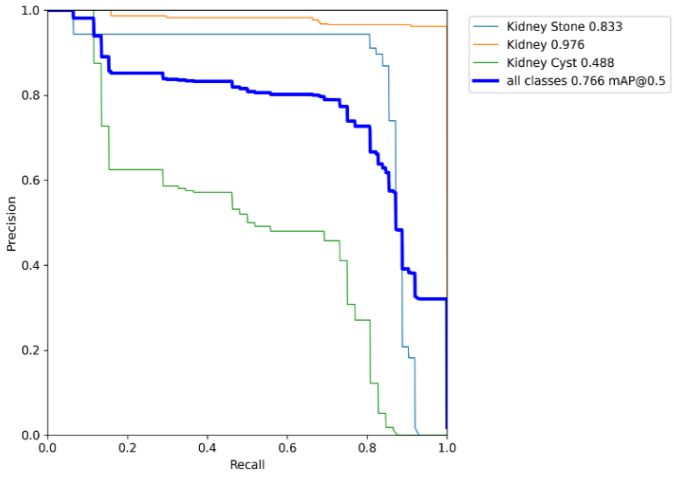

Figure 2. Obtained Precision-Recall curve by using YOLOv7 architecture design

Figure 3 shows the used number of 16 input images and the output images obtained by the YOLOv7 architecture design.

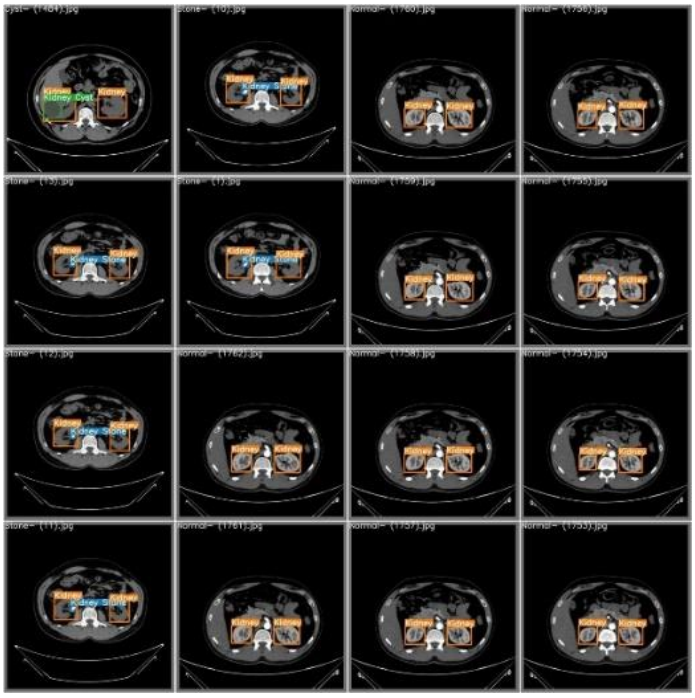

(a)

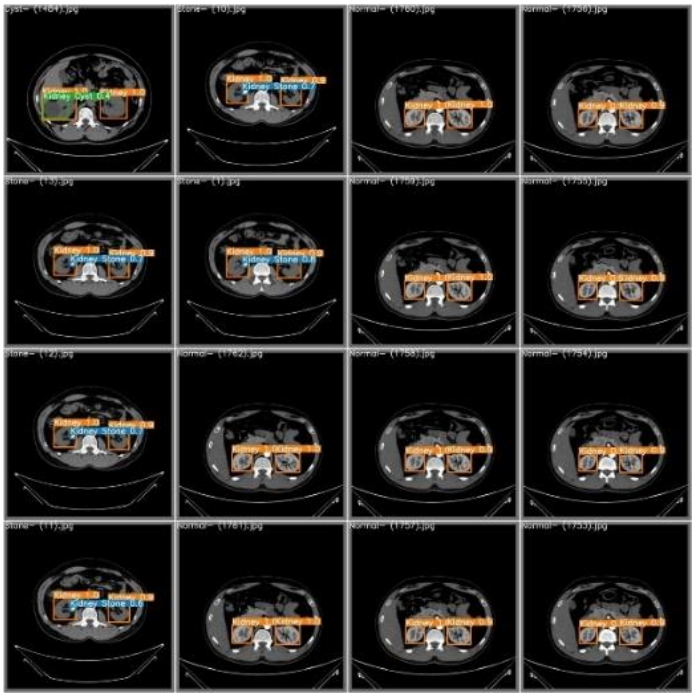

(b)

*Figure 3. **(a)** Labels of images in validation data set, **(b)** Predictions of images in validation data set achieved by YOLOv7*

4.2. Result Obtained By YOLOv7 Tiny

Table 2 represents the results obtained by using the YOLOv7 Tiny. The mAP50 of 61.8%, precision of 72.5%, sensitivity of 65.4% and F1 score of 68.7% values were achieved by YOLOv7 Tiny for all class. The mAP50 of 96.9%, precision of 91.2%, sensitivity of 98.3% and F1 score of 94.6% values were achieved by YOLOv7 Tiny for kidney class. The mAP50 of 70.3%, precision of 78.9%, sensitivity of 80.6% and F1 score of 79.7% values were achieved by YOLOv7 Tiny for kidney stone class. The mAP50 of 18.1%, precision of 47.3%, sensitivity of 17.3%

and F1 score of 25.3% values were achieved by YOLOv7 Tiny for kidney cyst class. The training period of the model took 1 hours and 17 minutes.

Table 2. Results obtained by YOLOv7 Tiny

Classes	mAP50	PRE	STV	F1-Score
Kidney	96.9%	91.2%	98.3%	94.6%
Kidney Stone	70.3%	78.9%	80.6%	79.7%
Kidney Cyst	18.1%	47.3%	17.3%	25.3%
Average	61.8%	72.5%	65.4%	68.7%

From Figure 4, considering the confusion matrix values, the classification accuracy values 0.87, 1.0, and 0.15 for kidney stones, kidney, and kidney cyst, respectively.

From Figure 5, the average precision-recall values were achieved as 0.669, 0.970, 0.139, 0.593for kidney stone, kidney, kidney cyst, and all classes.

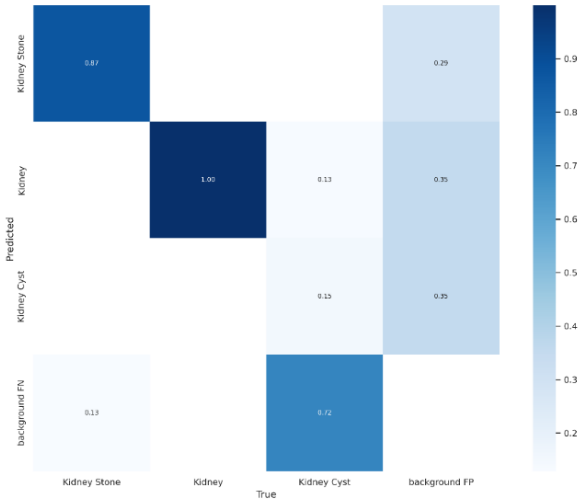

Figure 4. Obtained confusion matrix by using YOLOv7 Tiny architecture design

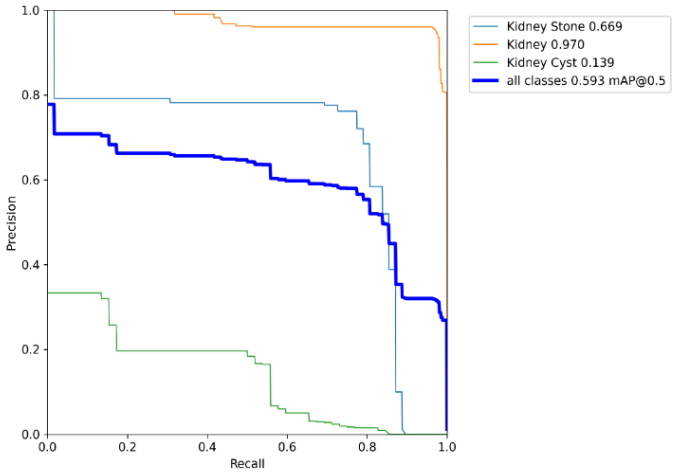

Figure 5. Obtained Precision-Recall curve by using YOLOv7 Tiny architecture design

Figure 6 shows the used number of 16 input images and the output images obtained by the YOLOv7 Tiny architecture design.

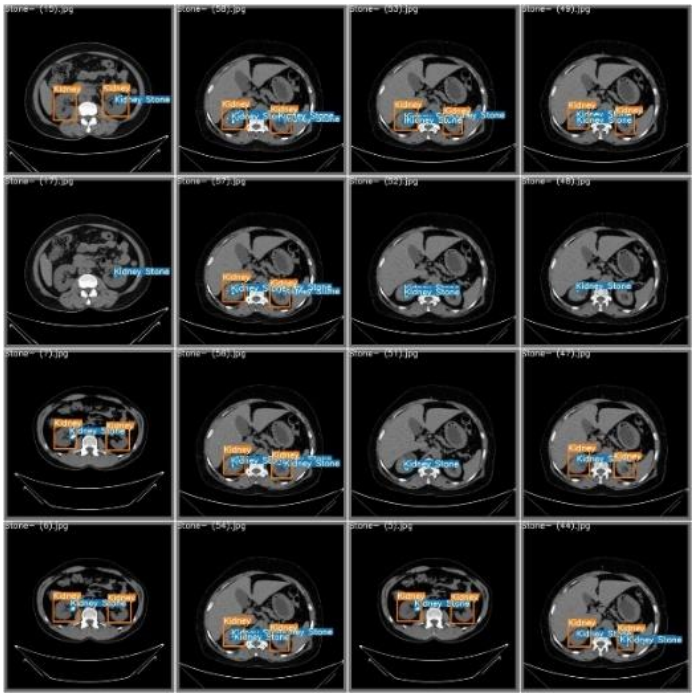

(a)

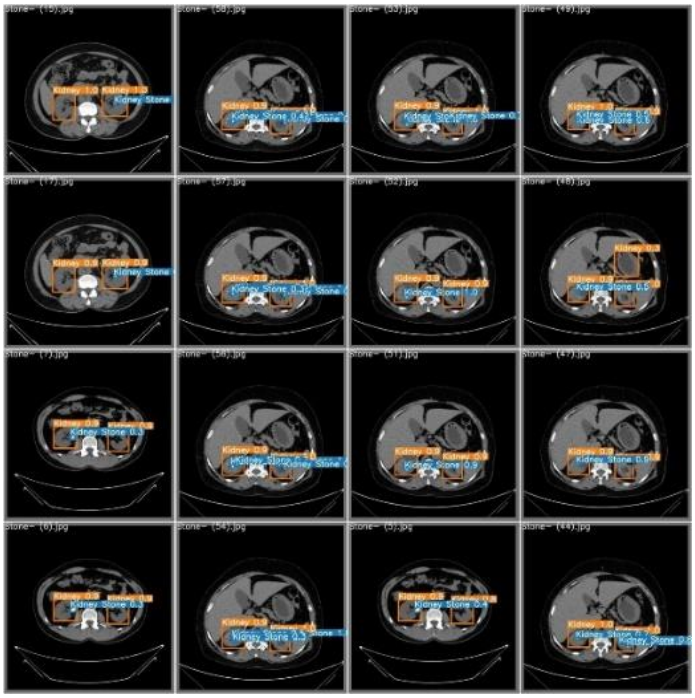

(b)

*Figure 6. **(a)** Labels of images in validation data set, **(b)** Predictions of images in validation data set achieved by YOLOv7 Tiny*

4.3. Outputs of xAI

In this study, Gradient Weighted Class Activation Mapping (Grad-CAM) was used to prove the performance of the outputs produced by the YOLOv7 architecture design, and to make it more clear and reliable by producing visual explanations for AI model. Consequently, the performance of the model made through visualizations was better displayed and interpreted. In addition, the model can more explainable distinguish between classes was proved. In the YOLOv7 model, target layers 102, 103 and 104

were used to output Grad-CAM. Grad-CAM outputs were created by using 2 input images for kidney cysts, 2 input images for kidney stones, and 2 input images for healthy kidneys. Figure 7, Figure 8, and Figure 9 show obtained xAI results for kidney cysts, kidney stones, and healthy kidneys, respectively. In Figures 7, 8 and 9 shows four main images: (i) the input image at the top left, (ii) the predict of the model at the top right, (iii) the Grad-CAM output of the kidney class at the bottom left, and (iv) the Grad-CAM output of the kidney stone or kidney cyst classes at the bottom right. If the kidney is healthy, the bottom right image is the Grad-CAM output of the kidney image but obtained from different output layer of model.

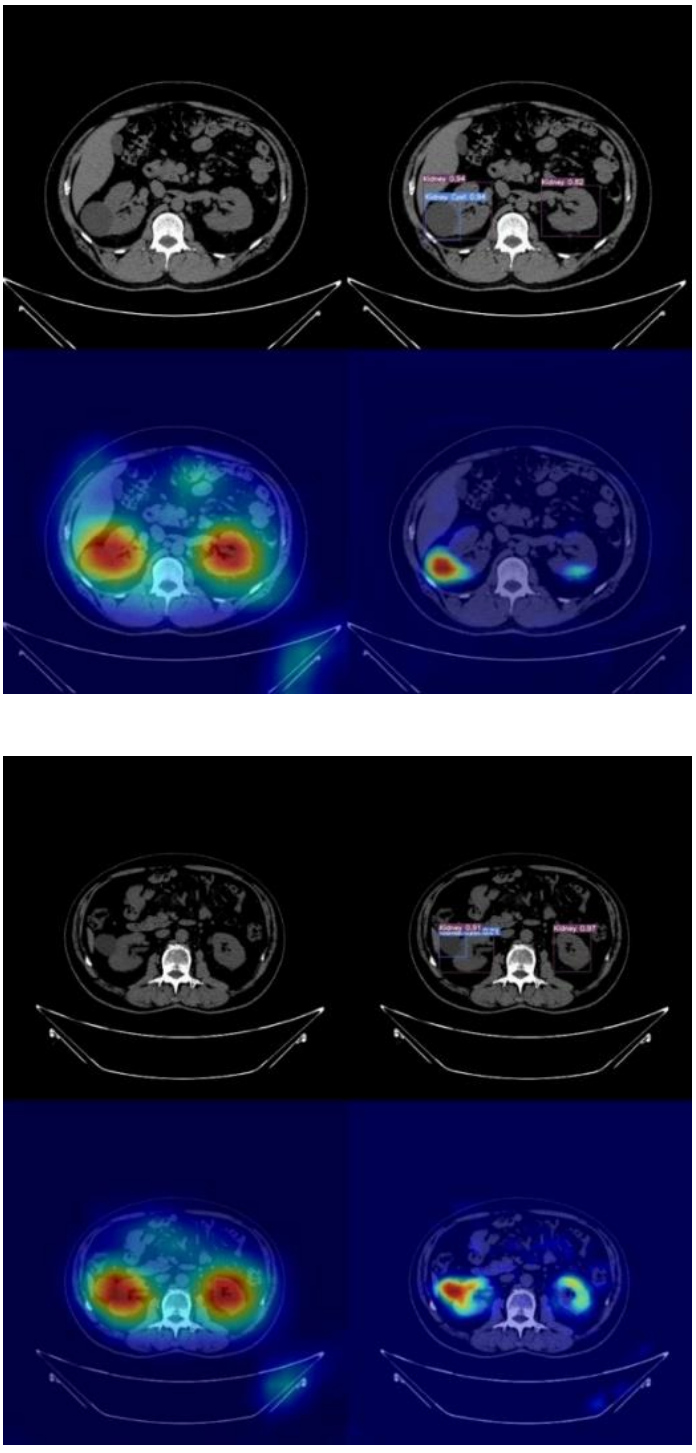

Figure 7. Outputs of xAI *for kidneys and kidney cysts using YOLOv7*

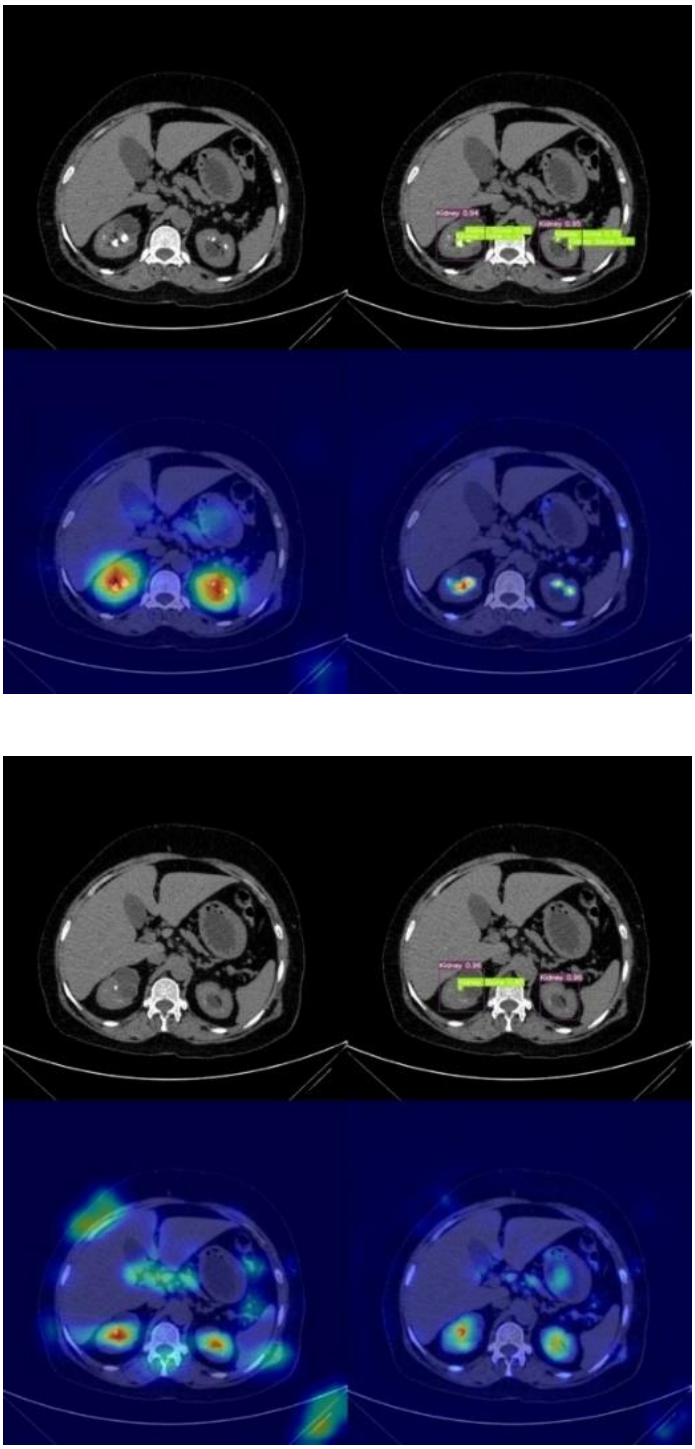

Figure 8. Outputs of xAI *for kidneys and kidney stones using YOLOv7*

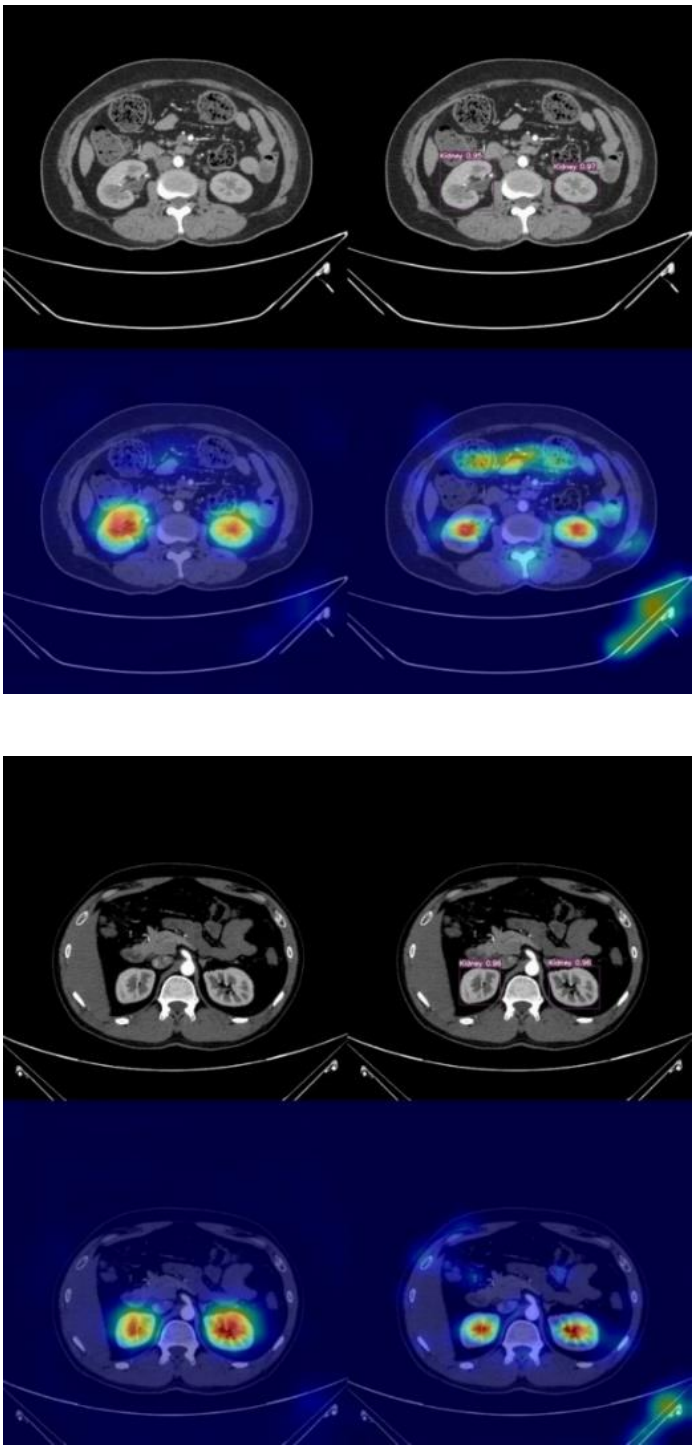

Figure 9. Outputs of xAI *for kidneys using YOLOv7*

5. Conclusion

In this study, YOLOv7 and YOLOv7 Tiny object detection networks were used to perform kidney, kidney stone, and kidney cyst. It is attempted to present a suggestion to other researchers on the detection performances of the object detection networks by comparing YOLOv7 and YOLOv7 Tiny networks. YOLOv7 object detection network achieved the mAP50 of 85%, precision of 88.2%, sensitivity of 82.9% and F1 score of 85.4% values were achieved by YOLOv7 for average of all classes. Consequently, with the help of the developed fully automatic kidney disease detection system, the workload of radiologists can be reduced.

6. Acknowledge

This paper has been prepared by AKGUN Computer Incorporated Company. We would like to thank AKGUN Computer Inc. for providing all kinds of opportunities and funds for the execution of this project.

References

Türk, C., Petřík, A., Sarica, K., Seitz, C., Skolarikos, A., Straub, M., & Knoll, T. (2016). EAU Guidelines on Diagnosis and Conservative Management of Urolithiasis. *European Urology*, *69*(3), 468–474. https://doi.org/10.1016/J.EURURO.2015.07.040

Stamatelou, K. K., Francis, M. E., Jones, C. A., Nyberg, L. M., & Curhan, G. C. (2003). Time trends in reported prevalence of kidney stones in the United States: 1976–1994. *Kidney International*, *63*(5), 1817–1823. https://doi.org/10.1046/J.1523-1755.2003.00917.X

Scales, C. D., Smith, A. C., Hanley, J. M., & Saigal, C. S. (2012). Prevalence of Kidney Stones in the United States. *European Urology*, *62*(1), 160–165. https://doi.org/10.1016/J.EURURO.2012.03.052

Fwu, C. W., Eggers, P. W., Kimmel, P. L., Kusek, J. W., & Kirkali, Z. (2013). Emergency department visits, use of imaging, and drugs for urolithiasis have increased in the United States. *Kidney International*, *83*(3), 479–486. https://doi.org/10.1038/KI.2012.419

Chewcharat, A., & Curhan, G. (2021). Trends in the prevalence of kidney stones in the United States from 2007 to 2016. *Urolithiasis*, *49*(1), 27–39. https://doi.org/10.1007/S00240-020-01210-W/TABLES/7

Weston, A. D., Korfiatis, P., Kline, T. L., Philbrick, K. A., Kostandy, P., Sakinis, T., Sugimoto, M., Takahashi, N., & Erickson, B. J. (2019). Automated Abdominal Segmentation of CT Scans for Body Composition Analysis Using Deep Learning. *Radiology*, *290*(3), 669–679. https://doi.org/10.1148/RADIOL.2018181432/ASSET/IMAGES/LARGE/RADIOL.2018181432.FIG5.JPEG

Ozturk, T., Talo, M., Yildirim, E. A., Baloglu, U. B., Yildirim, O., & Rajendra Acharya, U. (2020). Automated detection of COVID-19 cases using deep neural networks with X-ray images. *Computers in Biology and Medicine*, *121*, 103792. https://doi.org/10.1016/J.COMPBIOMED.2020.103792

Yan, K., Wang, X., Lu, L., & Summers, R. M. (2018). DeepLesion: automated mining of large-scale lesion annotations and universal lesion detection with deep learning. *Https://Doi.Org/10.1117/1.JMI.5.3.036501*, *5*(3), 036501. https://doi.org/10.1117/1.JMI.5.3.036501

Lin, Z., Cui, Y., Liu, J., Sun, Z., Ma, S., Zhang, X., & Wang, X. (2021). Automated segmentation of kidney and renal mass and automated detection of renal mass in CT urography using 3D U-Net-based deep convolutional neural network. *European Radiology*, *31*(7), 5021–5031. https://doi.org/10.1007/S00330-020-07608-9/FIGURES/6

Lin, D. T., Lei, C. C., & Hung, S. W. (2006). Computer-aided kidney segmentation on abdominal CT images. *IEEE Transactions on Information Technology in Biomedicine*, *10*(1), 59–65. https://doi.org/10.1109/TITB.2005.855561

Lin, Z., Cui, Y., Liu, J., Sun, Z., Ma, S., Zhang, X., & Wang, X. (2021). Automated segmentation of kidney and renal mass and automated detection of renal mass in CT urography using 3D U-Net-based deep convolutional neural network.

European Radiology, *31*(7), 5021–5031. https://doi.org/10.1007/S00330-020-07608-9/FIGURES/6

Baygin, M., Yaman, O., Barua, P. D., Dogan, S., Tuncer, T., & Acharya, U. R. (2022). Exemplar Darknet19 feature generation technique for automated kidney stone detection with coronal CT images. *Artificial Intelligence in Medicine*, *127*, 102274. https://doi.org/10.1016/J.ARTMED.2022.102274

Ruberto, C. Di, Loddo, A., Putzu, L., Stefano, A., Comelli, A., Li, D., Xiao, C., Liu, Y., Chen, Z., Hassan, H., Su, L., Liu, J., Li, H., Xie, W., Zhong, W., & Huang, B. (2022). Deep Segmentation Networks for Segmenting Kidneys and Detecting Kidney Stones in Unenhanced Abdominal CT Images. *Diagnostics 2022, Vol. 12, Page 1788*, *12*(8), 1788. https://doi.org/10.3390/DIAGNOSTICS12081788

Yildirim, K., Bozdag, P. G., Talo, M., Yildirim, O., Karabatak, M., & Acharya, U. R. (2021). Deep learning model for automated kidney stone detection using coronal CT images. *Computers in Biology and Medicine*, *135*, 104569. https://doi.org/10.1016/J.COMPBIOMED.2021.104569

Cui, Y., Sun, Z., Ma, S., Liu, W., Wang, X., Zhang, X., & Wang, X. (2021). Automatic Detection and Scoring of Kidney Stones on Noncontrast CT Images Using S.T.O.N.E. Nephrolithometry: Combined Deep Learning and Thresholding Methods. *Molecular Imaging and Biology*, *23*(3), 436–445. https://doi.org/10.1007/S11307-020-01554-0/FIGURES/6

Fu, X., Liu, H., Bi, X., & Gong, X. (2021). Deep-Learning-Based CT Imaging in the Quantitative Evaluation of Chronic Kidney Diseases. *Journal of Healthcare Engineering*, *2021*. https://doi.org/10.1155/2021/3774423

Islam, N., Hasan, M., Hossain, K., & Alam, G. R. (2022). Vision transformer and explainable transfer learning models for auto detection of kidney cyst , stone and tumor from CT - radiography. Scientific Reports, 1–14. https://doi.org/10.1038/s41598-022-15634-4

Make Sense. (n.d.). Retrieved August 28, 2022, from https://www.makesense.ai/

Gothane, S. (n.d.). *A Practice for Object Detection Using YOLO Algorithm Cite this paper A Practice for Object Detection Using YOLO Algorithm*. https://doi.org/10.32628/CSEIT217249

Dosilovic, F. K., Brcic, M., & Hlupic, N. (2018). Explainable artificial intelligence: A survey. *2018 41st International Convention on Information and Communication Technology, Electronics and Microelectronics, MIPRO 2018 - Proceedings*, 210–215. https://doi.org/10.23919/MIPRO.2018.8400040

Selvaraju, R. R., Cogswell, M., Das, A., Vedantam, R., Parikh, D., & Batra, D. (2017). *Grad-CAM: Visual Explanations From Deep Networks via Gradient-Based Localization* (pp. 618–626). http://gradcam.cloudcv.org

Selvaraju, R. R., Das, A., Vedantam, R., Cogswell, M., Parikh, D., Batra, D., & Tech, V. (2016). *Grad-CAM: Why did you say that?* https://doi.org/10.48550/arxiv.1611.07450